Organometallic Complexes for Nonlinear Optics. 3.[1] Molecular Quadratic Hyperpolarizabilities of Ene-, Imine-, and Azo-Linked Ruthenium σ-Acetylides: X-ray Crystal Structure of $Ru((E)\text{-}4,4'\text{-}C{\equiv}CC_6H_4CH{=}CHC_6H_4NO_2)(PPh_3)_2(\eta\text{-}C_5H_5)$

Ian R. Whittall and Mark G. Humphrey*

Department of Chemistry, Australian National University, Canberra, ACT 0200, Australia

André Persoons and Stephan Houbrechts

Centre for Research on Molecular Electronics and Photonics, Laboratory of Chemical and Biological Dynamics, University of Leuven, Celestijnenlaan 200D, B-3001 Leuven, Belgium

Received June 23, 1995[⊗]

The series of complexes $Ru((E)\text{-}4,4'\text{-}C{\equiv}CC_6H_4X{=}CHC_6H_4NO_2)(PR_3)_2(\eta\text{-}C_5H_5)$ (X = CH, R = Ph, **11a**; X = CH, R = Me, **11b**; X = N, R = Ph, **12a**; X = N, R = Me, **12b**) has been synthesized by reaction of $RuCl(PR_3)_2(\eta\text{-}C_5H_5)$ with $(E)\text{-}4,4'\text{-}HC{\equiv}CC_6H_4X{=}CHC_6H_4NO_2$ and deprotonation of the intermediate vinylidene complex. Complex **11a** has been structurally characterized; it is the first example of a donor-acceptor organometallic "extended" chromophore bearing the prototypical acceptor $-NO_2$ to be crystallographically studied. Molecular quadratic hyperpolarizabilities at 1.9 μm were evaluated computationally for the complexes above and imine- and azo-linked analogues by employing ZINDO with crystallographically obtained atomic coordinates. The results are consistent with a substantial increase in quadratic nonlinearity for (i) chain lengthening of the organometallic chromophore (replacing $4\text{-}C{\equiv}CC_6H_4NO_2$ by $(E)\text{-}4,4'\text{-}C{\equiv}CC_6H_4CH{=}CHC_6H_4NO_2$) and (ii) an azo linkage compared with an ene linkage (replacing $(E)\text{-}4,4'\text{-}C{\equiv}CC_6H_4CH{=}CHC_6H_4NO_2$ by $(E)\text{-}4,4'\text{-}C{\equiv}CC_6H_4N{=}NC_6H_4NO_2$). Little variation in computed response was found upon substituting an imine linkage for an ene linkage in the organometallic chromophore (replacing $(E)\text{-}4,4'\text{-}C{\equiv}CC_6H_4CH{=}CHC_6H_4NO_2$ by $(E)\text{-}4,4'\text{-}C{\equiv}CC_6H_4N{=}CHC_6H_4NO_2$ or $(E)\text{-}4,4'\text{-}C{\equiv}CC_6H_4\text{-}CH{=}NC_6H_4NO_2$). Molecular quadratic optical nonlinearities were determined experimentally for **11a**, **12a**, and $Ru(C{\equiv}CC_6H_4NO_2\text{-}4)(PR_3)_2(\eta\text{-}C_5H_5)$ (R = Ph, Me) by electric-field-induced second-harmonic generation (EFISH; **11a** and **12a** only) and hyper-Rayleigh scattering (HRS) techniques. EFISH-derived $\mu\beta_{1064}$ values for **11a** (9700×10^{-48} cm^5 esu^{-1}) and **12a** (5800×10^{-48} cm^5 esu^{-1}) are large compared to those for other organometallic complexes. Resonance-enhanced quadratic nonlinearities at 1.06 μm from HRS are large (1455×10^{-30} cm^5 esu^{-1}, **11a**; 840×10^{-30} cm^5 esu^{-1}, **12a**). Two-level-corrected values confirm a substantial increase in quadratic nonlinearity for chain lengthening but suggest a significant decrease in nonlinearity on replacing an ene linkage by an imine linkage; the latter is contrary to the ZINDO result, and the reasons for this are discussed.

Introduction

Although a great deal of work has been carried out in the investigation of the nonlinear optical properties of inorganic materials and organic molecules, the optical nonlinearities of organometallic complexes have been actively studied only recently.[2] Design criteria have been suggested to maximize organometallic nonlinear optical response, namely the incorporation of the metal into the plane of the π-system of the chromophore and the possible introduction of metal−carbon multiple-bond character.[3] With these ideas in mind, we have commenced an investigation into the optical nonlinearities of metal acetylide, vinylidene, carbene, and carbyne complexes and have recently reported results obtained with (aryldiazovinylidene)ruthenium salts[4] and (phenylacetylide)ruthenium complexes.[1] For the former, Kurtz powder measurements gave efficiencies on the order of that for urea, a common standard, despite the fact that the vinylidene complexes pack centrosymmetrically, a crystal alignment which should eliminate bulk quadratic nonlinearity; the observed response was assigned to large molecular nonlinearity coupled with some crystal mispacking or surface effects. Very recently we have employed ZINDO[5] to compute the quadratic molecular nonlinearity of [Ru(C=CPhN=N-

* To whom correspondence should be addressed.

⊗ Abstract published in *Advance ACS Abstracts,* March 15, 1996.

(1) Part 2: Whittall, I. R.; Humphrey, M. G.; Hockless, D. C. R.; Skelton, B. W.; White, A. H. *Organometallics* **1995**, *14*, 3970.

(2) For recent reviews see: (a) Nalwa, H. S. *Appl. Organomet. Chem.* **1991**, *5*, 349. (b) Long, N. J. *Angew. Chem., Int. Ed. Engl.* **1995**, *34*, 21.

(3) Calabrese, J. C.; Cheng, L.-T.; Green, J. C.; Marder, S. R.; Tam, W. *J. Am. Chem. Soc.* **1991**, *113*, 7227.

(4) Whittall, I. R.; Cifuentes, M. P.; Costigan, M. J.; Humphrey, M. G.; Goh, S. C.; Skelton, B. W.; White, A. H. *J. Organomet. Chem.* **1994**, *471*, 193.

(5) *ZINDO User Guide*; Biosym Technologies: San Diego, CA, 1994.

0276-7333/96/2315-1935$12.00/0

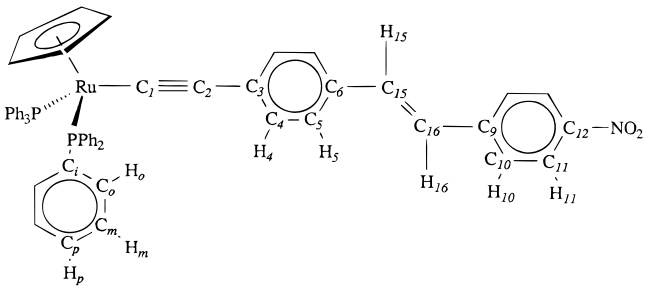

Figure 1. Numbering scheme for NMR spectral assignment of **11a**. Analogous schemes are used for **5**, **11b**, **12a**, and **12b**.

C_6H_4OMe-4)$(PPh_3)_2(\eta$-$C_5H_5)]^+$ and obtained a response 100 times that of urea,[6] a result which supports our assignment above. Our investigations with phenylacetylide complexes surveyed $Ru(C{\equiv}CC_6H_4R$-4)$(PR'_3)_2(\eta$-$C_5H_5)$ (R = H, NO_2; R′ = Ph, Me); computed molecular nonlinearities are consistent with increased response for (i) increased electron density at the metal center (replacing PPh_3 by PMe_3), (ii) increased acceptor strength of the aryl acetylide (replacing 4-H by 4-NO_2), and (iii) decreased M−C(acetylide) bond length. We have extended our studies with (acetylide)ruthenium complexes to those embracing longer chromophores and report herein our computed results for two-ring organometallic chromophores incorporating ene, imine, or azo linkages, together with electric field induced second-harmonic generation (EFISH) and hyper-Rayleigh scattering (HRS) experimentally determined molecular nonlinearities for the synthetically accessible ene− and imine−acetylide complexes and experimental data for the (nitrophenyl)acetylide complexes examined computationally in earlier work.[1]

Experimental Section

All organometallic reactions were carried out under an atmosphere of nitrogen with the use of standard Schlenk techniques; no attempt was made to exclude air during workup of organometallic products or while carrying out syntheses of organic compounds. Petroleum ether refers to a fraction of boiling point range 60−80 °C. The commercial reagents 4-bromobenzaldehyde, 4-bromonitrobenzene, 4-iodoaniline, and 4-nitrobenzaldehyde (Aldrich) were used as received. 4-Ethynylbenzaldehyde and 4-ethynylaniline were prepared similarly to literature methods.[7] $RuCl(L)_2(\eta$-$C_5H_5)$ (L = PPh_3, PMe_3) complexes were prepared by following literature methods.[8] Thin-layer chromatography was carried out using 7749 Kieselgel 60 PF_{254} silica (Merck). Microanalyses were carried out at the Research School of Chemistry, Australian National University. Infrared spectra were recorded using a Perkin-Elmer 1600 FT-IR spectrometer. ^1H, ^{13}C, and ^{31}P NMR spectra were recorded using a Bruker AC 300 or a Varian Gemini-300 FT NMR spectrometer and are referenced to residual $CHCl_3$ (7.24 ppm), $CDCl_3$ (77.0 ppm), and external 85% H_3PO_4 (0.0 ppm), respectively. UV−visible spectra were recorded using a Hitachi U-3200 spectrophotometer. NMR spectral assignments for **11a** follow the numbering scheme shown in Figure 1. Compounds **5**, **11b**, **12a**, and **12b** are numbered analogously.

Synthesis of $[Ph_3PCH_2C_6H_4NO_2$-4$][Br]$ (4). Triphenylphosphine (2.5 g, 9.5 mmol) and 4-nitrobenzyl bromide (3.1 g, 14 mmol) were refluxed in 50 mL of xylene for 2 h. The product precipitated during the reaction and upon cooling; it was collected by filtration and washed with petroleum ether, yielding 4.3 g (93%) of **4** as a white powder. Anal. Calcd for $C_{25}H_{21}NO_2PBr$: C, 62.78; H, 4.43; N, 2.93. Found: C, 62.36; H, 4.31; N, 2.79. ^1H NMR (δ; 300 MHz, $CDCl_3$): 5.91 (d, 2H, CH_2, J_{HP} = 6 Hz), 7.42 (dd, 2H, H_{10}, J_{HH} = 9 Hz, J_{HP} = 3 Hz), 7.60 (td, 6H, H_m, J_{HH} = 9 Hz, J_{HP} = 4 Hz), 7.72−7.87 (m, 11H, H_{11}, H_o, H_p). ^{13}C NMR (δ; 75 MHz, $CDCl_3$): 29.4 (d, CH_2, J_{CP} = 47 Hz), 117.0 (d, C_i, J_{CP} = 85 Hz), 122.9 (d, C_{11}, J_{CP} = 3 Hz), 129.9 (d, C_m, J_{CP} = 13 Hz), 132.7 (d, C_{10}, J_{CP} = 5 Hz), 134.3 (d, C_o, J_{CP} = 10 Hz), 134.9 (d, C_p, J_{CP} = 3 Hz), 135.6 (d, C_9, J_{CP} = 9 Hz), 147.1 (d, C_{12}, J_{CP} = 4 Hz). ^{31}P NMR (δ; 121 MHz, $CDCl_3$): 24.9. NMR spectral assignments for **4** follow the numbering scheme shown in Figure 2.

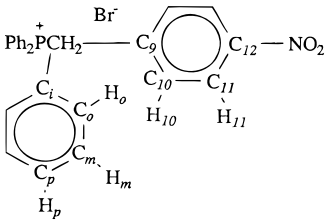

Figure 2. Numbering scheme for NMR spectral assignment of **4**.

Synthesis of (*E*)-4,4′-$HC{\equiv}CC_6H_4CH{=}CHC_6H_4NO_2$ (5). 4-Ethynylbenzaldehyde (0.36 g, 2.8 mmol) and (4-nitrobenzyl)-triphenylphosphonium bromide (1.3 g, 2.8 mmol) were dissolved in methanol (25 mL). A sodium methoxide in methanol solution (30 mL, 0.1 mol L^{-1}) was added, and the mixture was stirred for 2 h and then cooled by placing in ice. It was then filtered to afford a yellow powder of (*E*)-4,4′-$HC{\equiv}CC_6H_4CH{=}CHC_6H_4NO_2$ (150 mg, 22%). The filtrate contained triphenylphosphine oxide and the *Z* isomer, which on standing for days isomerized to, and precipitated more of, the *E* isomer, giving a total yield of up to 55%. Anal. Calcd for $C_{16}H_{11}NO_2$: C, 77.10; H, 4.45; N, 5.62. Found: C, 76.62; H, 4.46; N, 5.52. IR (CH_2Cl_2): ν(H−C≡) 3296 cm^{-1}. ^1H NMR (δ; 300 MHz, $CDCl_3$): 3.16 (s, 1H, HC≡), 7.14 (d, 1H, H_{15}, J_{HH} = 16 Hz), 7.23 (d, 1H, H_{16}, J_{HH} = 16 Hz), 7.49 (s, 4H, H_4 + H_5), 7.62 (d, 2H, H_9, J_{HH} = 9 Hz), 8.21 (d, 2H, H_{10}, J_{HH} = 9 Hz). ^{13}C NMR (δ; 75 MHz, $CDCl_3$): 78.6 (C_1), 83.4 (C_2), 122.4 (C_3), 124.2 (C_{11}), 126.9 (C_{10}), 127.0 (C_5), 127.3 (C_{15}), 132.3 (C_{16}), 132.6 (C_4), 136.6 (C_6), 143.4 (C_9), 147.0 (C_{12}). Crystals of **5** suitable for diffraction analysis were grown by slow evaporation of a $CHCl_3$ solution.[9] The *Z* isomer can be characterized by its ^1H NMR spectrum (δ; 300 MHz, $CDCl_3$): 3.09 (s, 1H, HC≡), 6.63 (d, 1H, H_{15}, J_{HH} = 12 Hz), 6.76 (d, 1H, H_{16}, J_{HH} = 12 Hz), 7.13 (d, 2H, H_4, J_{HH} = 9 Hz), 7.34 (d, 2H, H_{10}, J_{HH} = 9 Hz), 7.36 (d, 2H, H_5, J_{HH} = 9 Hz), 8.07 (d, 2H, H_{11}, J_{HH} = 9 Hz).

Synthesis of 4,4′-$HC{\equiv}CC_6H_4N{=}CHC_6H_4NO_2$ (9). 4-Ethynylaniline (100 mg, 0.85 mmol) and 4-nitrobenzaldehyde (130 mg, 0.86 mmol) were refluxed in ethanol (10 mL) for 2.5 h. The mixture was cooled and was then filtered. The product precipitated from the filtrate on addition of water and was extracted with ether and reduced, affording a yellow powder (213 mg, 63%). Anal. Calcd for $C_{15}H_{10}N_2O_2$: C, 71.98; H, 4.04; N, 11.20. Found: C, 72.31; H, 4.12; N, 10.93. IR (CH_2Cl_2): ν(H−C≡) 3294 cm^{-1}. ^1H NMR (δ; 300 MHz, $CDCl_3$): 3.12 (s, 1H, HC≡), 7.19 (d, 2H, H_4, J_{HH} = 9 Hz), 7.54 (d, 2H, H_5, J_{HH} = 9 Hz), 8.06 (d, 2H, H_{10}, J_{HH} = 9 Hz), 8.32 (d, 2H, H_{11}, J_{HH} = 9 Hz), 8.52 (s, 1H, =CH). ^{13}C NMR (δ; 75 MHz, $CDCl_3$): 78.0 (≡CH), 83.3 (C_2), 120.7 (C_3), 121.0 (C_5), 124.0 (C_{11}), 129.5 (C_{10}), 133.2 (C_4), 141.2 (C_9), 149.4 (C_{12}), 151.1 (C_6), 157.9 (=CH).

Synthesis of Ru((*E*)-4,4′-$C{\equiv}CC_6H_4CH{=}CHC_6H_4NO_2$)-$(PPh_3)_2(\eta$-$C_5H_5)$ (11a). $RuCl(PPh_3)_2(\eta$-$C_5H_5)$ (131 mg, 0.18 mmol) and (*E*)-4,4′-$HC{\equiv}CC_6H_4CH{=}CHC_6H_4NO_2$ (50 mg, 0.20

(6) Whittall, I. R.; Humphrey, M. G. Unpublished results.
(7) Takahashi, S.; Kuroyama, Y.; Sonogashira, K.; Hagihara, N. *Synthesis* **1980**, 627.
(8) (a) Bruce, M. I.; Hameister, C.; Swincer, A. G.; Wallis, R. C. *Inorg. Synth.* **1982**, *21*, 78. (b) Bruce, M. I.; Wong, F. S. *J. Organomet. Chem.* **1981**, *210*, C5.

(9) Full details of the X-ray crystallographic study of **5** are being reported elsewhere: Whittall, I. R.; Humphrey, M. G.; Hockless, D. C. R. *Acta Crystallogr., Sect. C*, submitted for publication.

mmol) were refluxed in MeOH (10 mL) for 30 min and then cooled. A solution of sodium methoxide in methanol (4 mL, 0.1 mol L^{-1}) was added and then the solvent volume reduced to 5 mL under reduced pressure. Filtration afforded the product as a red microcrystalline powder (169 mg, 92%). Anal. Calcd for $C_{57}H_{45}NO_2P_2Ru$: C, 72.91; H, 4.83; N, 1.49. Found: C, 73.39; H, 4.61; N, 1.42. IR (cyclohexane): ν(C≡C) 2071 cm^{-1}. IR (CH_2Cl_2): ν(C≡C) 2064 cm^{-1}. ^1H NMR (δ; 300 MHz, $CDCl_3$): 4.32 (s, 5H, C_5H_5), 7.00 (d, 1H, H_{15}, J_{HH} = 16 Hz), 7.08 (t, 12H, H_m, J_{HH} = 7 Hz), 7.19 (m, 7H, H_{16} + H_p), 7.46 (m, 12H, H_o), 7.57 (d, 2H, H_{10}, J_{HH} = 9 Hz), 8.18 (d, 2H, H_{11}, J_{HH} = 9 Hz). ^{13}C NMR (δ; 75 MHz, $CDCl_3$): 85.3 (C_5H_5), 115.8 (C_2), 123.6 (C_{15}), 124.2 (C_{11}), 124.2 (t, C_1, J_{CP} = 25 Hz), 126.4 (C_5), 126.7 (C_{10}), 127.2 (t, C_m, J_{CP} = 5 Hz), 128.5 (C_p), 130.6 (C_3), 130.9 (C_4), 131.5 (C_6), 133.8 (t, C_o, J_{CP} = 5 Hz, + C_{16}), 138.7 (m, C_i), 144.7 (C_9), 146.1 (C_{12}). ^{31}P NMR (δ; 121 MHz, $CDCl_3$): 51.1. Crystals of **11a** suitable for diffraction analysis were grown by slow diffusion of methanol into dichloromethane solution at 20 °C.

Synthesis of Ru((*E*)-4,4′-C≡CC_6H_4CH═CH$C_6H_4NO_2$)(PMe_3)$_2$(η-C_5H_5) (11b). Ru(Cl)(PMe_3)$_2$(η-C_5H_5) (100 mg, 0.28 mmol) and (*E*)-4,4′-HC≡CC_6H_4CH═CH$C_6H_4NO_2$ (70 mg, 0.28 mmol) were refluxed in MeOH (10 mL) for 30 min, and the solution was cooled. A solution of sodium methoxide in methanol (6 mL, 0.1 mol L^{-1}) was added and then the solvent removed under reduced pressure. The residue was dissolved in CH_2Cl_2; this solution was passed through a short alumina column and then purified using thin-layer chromatography, affording a purple solid (85 mg, 53%). Anal. Calcd for $C_{27}H_{33}NO_2P_2Ru$: C, 57.23; H, 5.88; N, 2.47. Found: C, 57.92; H, 5.74; N, 1.73. IR (cyclohexane): ν(C≡C) 2068 cm^{-1}. IR (CH_2Cl_2): ν(C≡C) 2053 cm^{-1}. ^1H NMR (δ; 300 MHz, $CDCl_3$): 1.49 (m, 18H, Me), 4.71 (s, 5H, C_5H_5), 6.96 (d, 1H, H_{15}, J_{HH} = 16 Hz), 7.18 (d, 1H, H_{16}, J_{HH} = 16 Hz), 7.18 (d, 2H, H_4, J_{HH} = 8 Hz), 7.30 (d, 2H, H_5, J_{HH} = 8 Hz), 7.55 (d, 2H, H_{10}, J_{HH} = 9 Hz), 8.16 (d, 2H, H_{11}, J_{HH} = 9 Hz). ^{13}C NMR (δ; 75 MHz, $CDCl_3$): 23.1 (m, Me), 81.1 (C_5H_5), 109.4 (C_2), 123.4 (C_{15}), 124.1 (C_{11}), 126.7 (C_{10}), 129.3 (t, C_1, J_{CP} = 25 Hz), 130.4 (C_3), 131.0 (C_4), 131.4 (C_6), 133.7 (C_{16}), 144.6 (C_9), 146.0 (C_{12}). ^{31}P NMR (δ; 121 MHz, $CDCl_3$): 13.7.

Synthesis of Ru(4,4′-C≡CC_6H_4N═CH$C_6H_4NO_2$)(PPh_3)$_2$(η-C_5H_5) (12a). The preparation of Ru(4,4′-C≡CC_6H_4N═CH-$C_6H_4NO_2$)(PPh_3)$_2$(η-C_5H_5) (**12a**) was analogous to the preparation of (**11b**) using Ru(Cl)(PPh_3)$_2$(η-C_5H_5) (200 mg, 0.28 mmol) and 4,4′-HC≡CC_6H_4N═CH$C_6H_4NO_2$ (**9**; 105 mg, 0.30 mmol), affording a purple solid (133 mg, 51%). Anal. Calcd for $C_{56}H_{44}N_2O_2P_2Ru$: C, 71.56; H, 4.72; N, 2.98. Found: C, 70.98; H, 4.73; N, 2.85. IR (cyclohexane): ν(C≡C) 2073 cm^{-1}. IR (CH_2Cl_2): ν(C≡C) 2066 cm^{-1}. ^1H NMR (δ; 300 MHz, $CDCl_3$): 4.32 (s, 5H, C_5H_5), 7.07 (t, 12H, H_m, J_{HH} = 7 Hz), 7.18 (t, 10H, H_p, J_{HH} = 7 Hz, + H_4, H_5), 7.46 (m, 12H, H_o), 8.03 (d, 2H, H_{10}, J_{HH} = 9 Hz), 8.29 (d, 2H, H_{11}, J_{HH} = 9 Hz), 8.57 (s, 1H, ═CH). ^{13}C NMR (δ; 75 MHz, $CDCl_3$): 85.3 (C_5H_5), 115.2 (C_2), 121.2 (C_5), 122.5 (t, C_1, J_{CP} = 25 Hz), 123.9 (C_{11}), 127.2 (t, C_m, J_{CP} = 5 Hz), 128.4 (C_p), 128.9 (C_{10}), 130.4 (C_3), 131.3 (C_4), 133.8 (t, C_o, J_{CP} = 5 Hz), 142.3 (C_9), 145.2 (C_6), 148.7 (C_{12}), 153.8 (═CH). ^{31}P NMR (δ; 121 MHz, $CDCl_3$): 51.1.

Synthesis of Ru(4,4′-C≡CC_6H_4N═CH$C_6H_4NO_2$)(PMe_3)$_2$(η-C_5H_5) (12b). The preparation of Ru(4,4′-C≡CC_6H_4-N═CH$C_6H_4NO_2$)(PMe_3)$_2$(η-C_5H_5) (**12b**) was analogous to the preparation of **11b** using Ru(Cl)(PMe_3)$_2$(η-C_5H_5) (50 mg, 0.14 mmol) and 4,4′-HC≡CC_6H_4N═CH$C_6H_4NO_2$ (**9**; 42 mg, 0.17 mmol), affording a purple solid (45 mg, 57%). Anal. Calcd for $C_{26}H_{32}N_2O_2P_2Ru$: C, 55.02; H, 5.68; N, 4.94. Found: C, 55.62; H, 5.54; N, 3.87. IR (cyclohexane): ν(C≡C) 2071 cm^{-1}. IR (CH_2Cl_2): ν(C≡C) 2055 cm^{-1}. ^1H NMR (δ; 300 MHz, $CDCl_3$): 1.50 (m, 18H, Me), 4.71 (s, 5H, C_5H_5), 7.13 (d, 2H, H_5), 7.22 (d, 2H, H_4), 8.01 (d, 2H, H_{10}, J_{HH} = 9 Hz), 8.27 (d, 2H, H_{11}, J_{HH} = 9 Hz), 8.54 (s, 1H, ═CH). ^{13}C NMR (δ; 75 MHz, $CDCl_3$): 23.2 (m, Me), 81.1 (C_5H_5), 108.8 (C_2), 121.2 (C_5), 124.0 (C_{11}), 127.2 (t, C_1, J_{CP} = 25 Hz), 129.0 (C_{10}), 130.3 (C_3), 131.5 (C_4), 142.3 (C_9), 145.0 (C_6), 148.8 (C_{12}), 153.8 (═CH). ^{31}P NMR (δ; 121 MHz, $CDCl_3$): 13.7.

X-ray Crystallography. A unique diffractometer data set was measured within the specified $2\theta_{max}$ limit (monochromatic radiation; $\omega-2\theta$ scan mode), yielding N independent reflections. N_o of these with $I > 3\sigma(I)$ were considered "observed" and used in the full-matrix least-squares refinements after absorption correction. Anisotropic thermal parameters were refined for the non-hydrogen atoms; (x, y, z, U_{iso})$_H$ were included constrained at estimated values. Conventional residuals R and R_w on $|F|$ at convergence are given. Neutral atom complex scattering factors were used. Data reduction was performed using the Xtal 3.2[10] program system, with other calculations performed using the teXsan[11] program system. Pertinent results are given in Figure 4 and Table 1; material deposited in the Supporting Information comprises atomic coordinates, thermal parameters, and full non-hydrogen geometries. Individual variants are noted in Table 1.

Computational Details. Results were obtained using ZINDO[5] (June 1994 version) from Biosym Technologies, San Diego, CA, implemented on a Silicon Graphics INDY workstation without parameter manipulation or basis function alteration. Calculations used crystallographically derived atomic coordinates[12] as input data. CI calculations included single excitations; basis set sizes were increased progressively for all calculations until convergence ($\pm 2 \times 10^{-30}$ cm^5 esu^{-1}) in the computed β_{vec} value was reached (200−300 excited configurations for organometallics, 100 for the organic compounds).

HRS Measurements. An injection-seeded Nd:YAG laser (Q-switched Nd:YAG Quanta Ray GCR5, 1064 nm, 8 ns pulses, 10 pps) was focused into a cylindrical cell (7 mL) containing the sample. The intensity of the incident beam was varied by rotation of a half-wave plate placed between crossed polarizers. Part of the laser pulse was sampled by a photodiode to measure the vertically polarized incident light intensity. The frequency-doubled light was collected by an efficient condenser system under 90° and detected by a photomultiplier. The harmonic scattering and linear scattering were distinguished by appropriate filters; gated integrators were used to obtain intensities of the incident and harmonic scattered light. All measurements were performed in THF using *p*-nitroaniline ($\beta = 21.4 \times 10^{-30}$ cm^5 esu^{-1})[13] as a reference. Further details of the experimental procedure have been reported elsewhere.[14]

Other Measurements. EFISH measurements were carried out on tetrahydrofuran solutions of graded concentrations using standard procedures.[15] Dipole moments were determined by standard methods.[16]

Results and Discussion

Synthesis of Acetylenes. Acetylenes required for the acetylide synthesis were prepared by extension of well-established organic synthetic procedures. Thus, (*E*)-4,4′-HC≡CC_6H_4CH═CH$C_6H_4NO_2$ (**5**) was formed by coupling 4-ethynylbenzaldehyde and (4-nitrobenzyl)-triphenylphosphonium bromide by standard Wittig

(10) Hall, S. R.; Flack, H. D.; Stewart, J. M. *The XTAL 3.2 Reference Manual*; Universities of Western Australia, Geneva, and Maryland, 1992.
(11) teXsan: Single Crystal Structure Analysis Software, Version 1.6c; Molecular Structure Corporation: The Woodlands, TX, 1993.
(12) Compound **5**: Reference 9. Compound **11a**: This work. Ru(Cl)(PPh_3)$_2$(η-C_5H_5): Bruce, M. I.; Wong, F. S.; Skelton, B. W.; White, A. H. *J. Chem. Soc., Dalton Trans.* **1981**, 1398.
(13) Stähelin, M., Burland, D. M.; Rice, J. E. *Chem. Phys. Lett.* **1992**, *191*, 245.
(14) (a) Clays, K.; Persoons, A. *Rev. Sci. Instrum.* **1992**, *63*, 3285. (b) Hendrickx, E.; Persoons, A.; Dehu, C.; Bredas, J. L. *J. Am. Chem. Soc.* **1995**, *117*, 3547.
(15) Cheng, L.-T.; Tam, W.; Stevenson, S. H.; Meredith, G. R.; Rikken, G.; Marder, S. R. *J. Phys. Chem.* **1991**, *95*, 10631.
(16) Guggenheim, E. A. *Trans. Faraday Soc.* **1949**, *45*, 203.

Scheme 1[a]

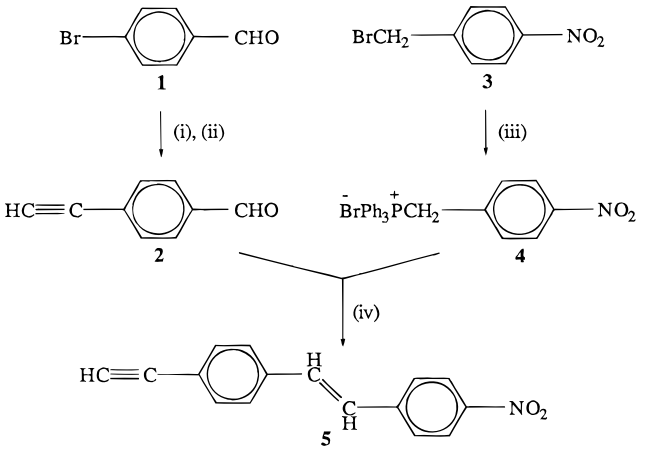

[a] Legend: (i) $Me_3SiC{\equiv}CH$, $PdCl_2(PPh_3)_2$, CuI, NEt_3; (ii) K_2CO_3, MeOH; (iii) PPh_3, xylene; (iv) NaOMe, MeOH.

Scheme 2[a]

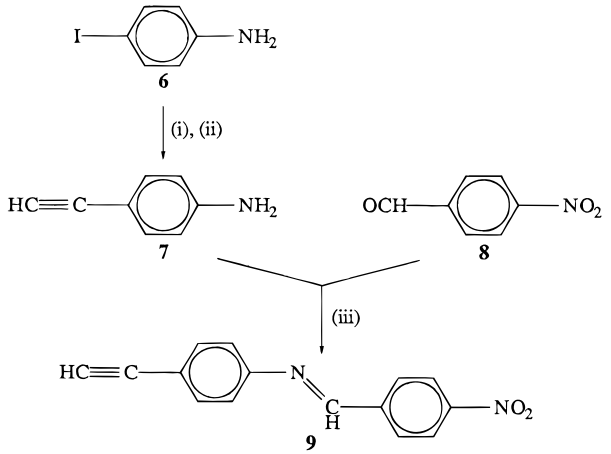

[a] Legend: (i) $Me_3SiC{\equiv}CH$, $PdCl_2(PPh_3)_2$, CuI, NEt_3; (ii) K_2CO_3, MeOH; (iii) refluxing EtOH.

methods (Scheme 1) and (*E*)-4,4′-$HC{\equiv}CC_6H_4N{=}CHC_6H_4NO_2$ (**9**) by a Schiff base condensation of 4-ethynylaniline with 4-nitrobenzaldehyde (Scheme 2). Attempts to isolate the "reverse" iminoacetylene (*E*)-4,4′-$HC{\equiv}CC_6H_4CH{=}NC_6H_4NO_2$ were unsuccessful, as it readily hydrolyzes to the starting materials 4-$HC{\equiv}CC_6H_4CHO$ and 4-$H_2NC_6H_4NO_2$. Both new acetylenes were characterized by a combination of IR and ^1H and ^{13}C NMR spectra and satisfactory microanalyses; a solid-state structural determination of **5** confirmed its identity.[9]

Syntheses and Characterization of (Acetylide)ruthenium Complexes. The ruthenium acetylide synthetic methodology has been described elsewhere[17] (Scheme 3).

Complexes **11a**, **11b**, **12a**, and **12b** were characterized by IR and ^1H, ^{13}C, and ^{31}P NMR spectroscopy and satisfactory microanalyses; complexes **11b**, **12a**, and **12b** have limited stability, decomposing slowly at room temperature in the solid state under an inert atmosphere. Characteristic $\nu(C{\equiv}C)$ signals in the solution IR spectra show some solvent dependence (2071 (cyclohexane), 2064 (CH_2Cl_2) cm^{-1}, **11a**; 2068, 2053 cm^{-1}, **11b**; 2073, 2066 cm^{-1}, **12a**; 2071, 2055 cm^{-1}, **12b**); the shift to lower energy in the more polar solvent is consistent with increased stabilization of a charge-separated vinylidene contributor (Ru—C≡C—Ar ↔ $Ru^+{=}C{=}C{=}Ar^-$). The ^1H (4.32 ppm, **11a**; 4.71 ppm, **11b**; 4.32 ppm, **12a**; 4.71 ppm, **12b**) and ^{13}C NMR spectra (85.3 ppm, **11a**; 81.1 ppm, **11b**; 85.3 ppm, **12a**; 81.1 ppm, **12b**) contain characteristic resonances for the cyclopentadienyl groups, whose chemical shifts are a function of the phosphine but do not vary with these subtle changes in acetylide. The metal-bound acetylide α-carbon (124.2 ppm, **11a**; 129.3 ppm, **11b**; 122.5 ppm, **12a**; 127.2 ppm, **12b**) shows the same phosphine dependence (5 ppm downfield shift on replacing triphenylphosphine by trimethylphosphine) as we observed previously for the analogous (4-nitrophenyl)- and (4-protiophenyl)acetylide complexes[1] and a smaller variation (1.7 ppm) on acetylide modification. The *β*-carbon of the acetylide group (115.8 ppm, **11a**; 109.4 ppm, **11b**; 115.2 ppm, **12a**; 108.8 ppm, **12b**) similarly shows a large (6.4 ppm) phosphine dependence and small (0.6 ppm) acetylide dependence. Mulliken population analyses of complexes **11a** and **12a** employing ZINDO[5] are consistent with the spectral data (little or no effect on important resonances upon bridge replacement) and show that the effect on the ground-state charge distribution of replacing an ene by an imine linkage is restricted to atoms adjacent to the heteroatom, a result which is also true for the "reverse" imine- and azo-linked analogues discussed below (Figure 3).

Scheme 3

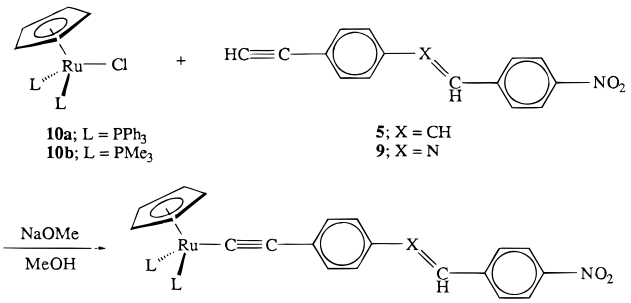

	L	X	isomer
11a	PPh_3	CH	(*E*)
11b	PMe_3	CH	(*E*)
12a	PPh_3	N	(*E*)
12b	PMe_3	N	(*E*)

Structural Characterization of 11a. We have completed X-ray diffraction studies on **11a** and its precursor acetylene **5** (full details of the latter are reported elsewhere[9]) to examine the resultant data for any differences due to coordination, to compare **11a** with the "one-ring" (acetylide)ruthenium complexes we have crystallographically characterized previously,[1,18] and to provide reliable input data for the computational work detailed below. Crystallographic data for **11a** are collected in Table 1, with selected bond lengths and angles given in Table 2; an ORTEP plot is displayed in Figure 4.

Ru—P distances for **11a** are comparable to those in $Ru(C{\equiv}CC_6H_4NO_2\text{-}4)(PPh_3)_2(\eta\text{-}C_5H_5)$ (2.297(2), 2.301(2)

(17) Bruce, M. I.; Wallis, R. C. *Aust. J. Chem.* **1979**, *32*, 1471.

(18) Bruce, M. I.; Humphrey, M. G., Snow, M. R.; Tiekink, E. R. T. *J. Organomet. Chem.* **1986**, *314*, 213.

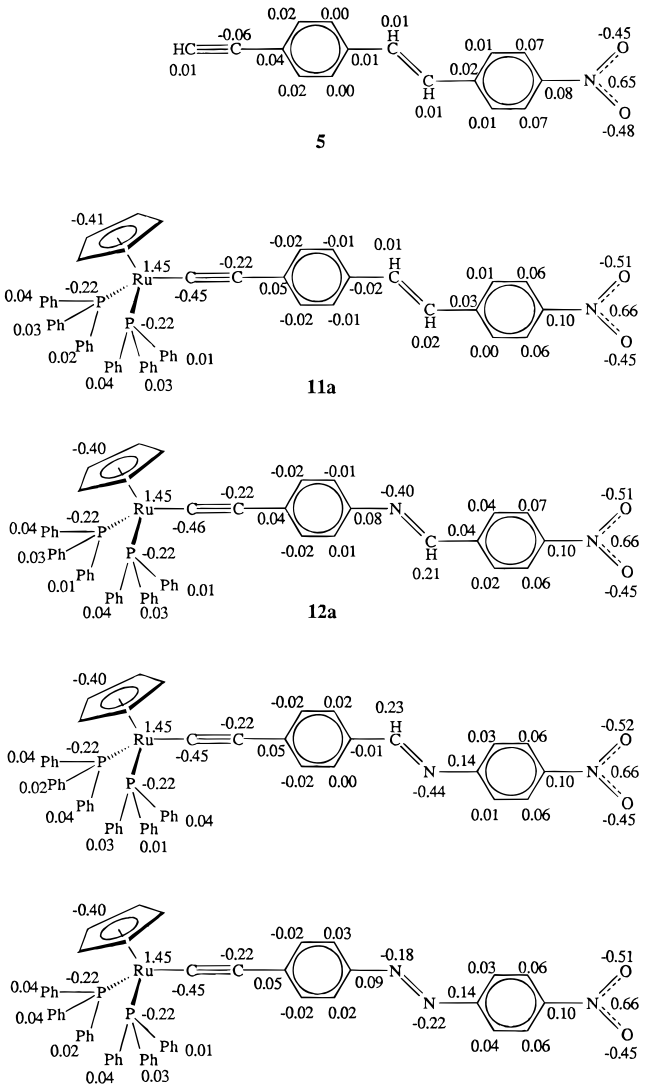

Figure 3. Mulliken analyses.

Table 1. Crystallographic Data for 11a

chem formula	$C_{57}H_{45}NO_2P_2Ru$
fw	939.01
space group	$P2_1/n$ (No. 14)
a, Å	11.092(4)
b, Å	19.445(9)
c, Å	21.09(1)
β, deg	100.56(4)
V, Å^3	4470(3)
ρ_{calcd}, g cm^{-3}	1.395
Z	4
diffractometer	Philips PW 1100/20
radiation/λ, Å	Mo Kα/0.71073
μ, cm^{-1}	4.68
T, K	295
specimen size, mm	0.3 × 0.2 × 0.15
T (min, max)	0.94, 0.95
$2\theta_{max}$, deg	50
N	7849
N_o	3707
R	0.048
R_w	0.027
decay cor	linear (3%)

Å)[1] and substantially longer than those in Ru(C≡CPh)-$(PPh_3)_2(\eta$-$C_5H_5)$ (2.229(3), 2.228(3) Å).[18] In the absence of any significant steric differences, this can be ascribed to substantial electronic differences deriving from the presence of the strong acceptor acetylide ligands. The Ru−C(1) vector is comparable in length to all other (cyclopentadienyl)bis(phosphine)ruthenium acetylides

Table 2. Important Bond Lengths (Å) and Angles (deg) for Complex 11a

Ru−P(1)	2.292(2)	C(6)−C(7)	1.383(8)
Ru−P(2)	2.280(2)	C(6)−C(15)	1.476(8)
Ru−(η-C_5H_5)	2.236(6)	C(7)−C(8)	1.372(8)
	2.235(7)	C(9)−C(10)	1.363(9)
	2.222(7)	C(9)−C(14)	1.380(9)
	2.219(7)	C(9)−C(16)	1.455(8)
	2.228(8)	C(10)−C(11)	1.372(10)
Ru−C(1)	2.008(6)	C(11)−C(12)	1.33(1)
C(1)−C(2)	1.199(7)	C(12)−C(13)	1.35(1)
C(2)−C(3)	1.438(8)	C(12)−N(1)	1.44(1)
C(3)−C(4)	1.394(8)	C(13)−C(14)	1.385(10)
C(3)−C(8)	1.376(8)	C(15)−C(16)	1.302(8)
C(4)−C(5)	1.370(8)	N(1)−O(1)	1.24(1)
C(5)−C(6)	1.385(8)	N(1)−O(2)	1.18(1)
Ru−C(1)−C(2)	174.2(6)	C(6)−C(15)−C(16)	129.1(7)
P(1)−Ru−P(2)	99.01(6)	C(9)−C(16)−C(15)	129.1(8)
C(1)−Ru−P(1)	91.3(2)	C(12)−N(1)−O(1)	116(1)
C(1)−Ru−P(2)	89.6(2)	C(12)−N(1)−O(2)	119(1)
C(1)−C(2)−C(3)	177.6(7)	O(1)−N(1)−O(2)	124(1)

we have crystallographically examined and substantially shorter than that in most other ruthenium σ-acetylides.[1] The C(1)-C(2) bond is lengthened slightly in **11a** (1.199(7) Å) compared with that in **5** (1.175(3) Å) and the C(2)−C(3) interaction shortened marginally (1.438(8) Å, **11a**; 1.447(3) Å, **5**), although both differences are within experimental errors. Ru−C(1)−C(2) and C(1)−C(2)−C(3) angles are essentially linear (and the latter are comparable for **5** (178.7(2)°) and **11a** (177.6(7)°)). Bond and angle data for the rings and ethylene bridge in **5** and **11a** are virtually identical; the only substantial difference (∠C(9)−C(16)−C(15) = 124.1(2)° **(5)**, 129.1(8)° **(11a)**) may be related to the dihedral angle between the phenylene units being greater for **5** (47.5°) than for **11a** (12.5°), which would tend to minimize H(10)−H(16) repulsion and favor an idealized sp^2 geometry (120°).

Quadratic Hyperpolarizabilities. The linear optical absorption spectra for donor−acceptor acetylide complexes of the type considered here have a low energy MLCT transition (Table 3); this undergoes a red shift on chain lengthening, with the lowest energy absorption for the imine-linked acetylide complex (**12a**). ZINDO reproduces the red shift of the MLCT transition, although absolute values are not reproduced. We have demonstrated previously that these bands undergo substantial positive solvatochromism, indicating a significant dipole moment change between ground and excited states,[1] an indicator of enhanced quadratic nonlinearity.

Complexes **11a** and **12a** were examined by EFISH (Table 3). The experimentally obtained $\mu\beta_{1064}$ values, 9700 × 10^{-48} and 5800 × 10^{-48} esu, respectively, are resonance-enhanced but are large in magnitude compared to previously reported organometallic data (the $\mu\beta$ product is the relevant parameter to assess poled polymer potential).[19] Experimentally determined dipole moments of 6.7 and 7.6 D, respectively, afford β_{vec} values consistent with those obtained by HRS. As the values of β measured by EFISH and HRS are equal, and considering that these techniques determine different combinations of tensor components, we conclude that there is only one dominating tensor component and that, therefore, the β value as determined by HRS can also

(19) Di Bella, S.; Fragalà, I.; Ledoux, I.; Marks, T. J. *J. Am. Chem. Soc.* **1995**, *117*, 9481.

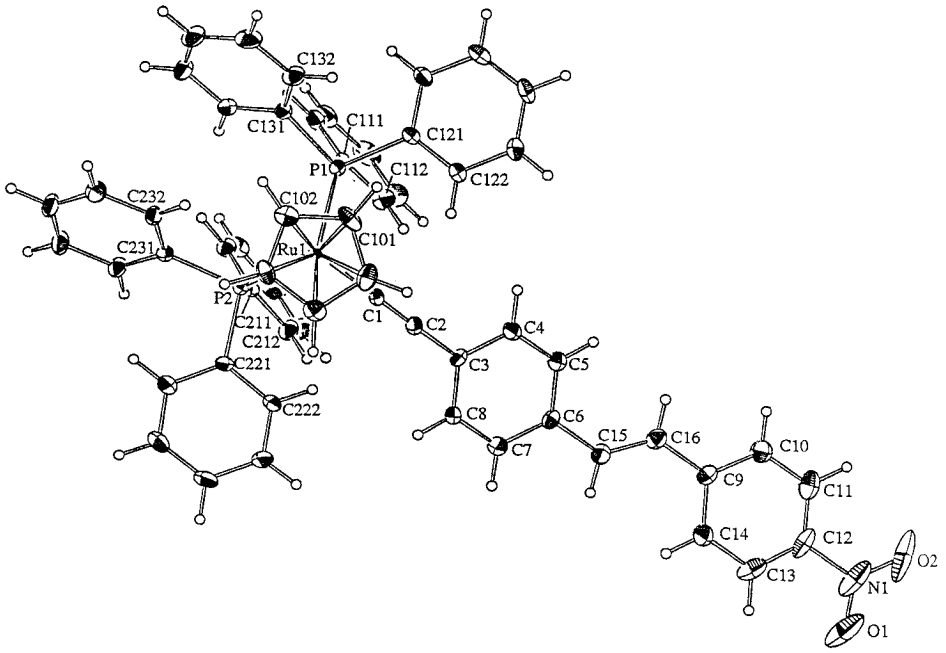

Figure 4. Molecular structure and atomic labeling scheme for **11a**. Thermal ellipsoids at the 20% level are shown for the non-hydrogen atoms; hydrogen atoms have arbitrary radii of 0.1 Å.

Table 3. Experimental[a] and ZINDO-Derived Linear Optical Spectroscopic and Nonlinear Optical Response Parameters

	λ_{max} (nm)		μ_g (D)		β_{vec} (10^{-30} cm^5 esu^{-1})		
compound	exptl ($\epsilon \times 10^{-4}$)	calcd	exptl	calcd	exptl[b]	corrected[c]	calcd[d]
(*E*)-4,4′-HC≡CC_6H_4CH═$CHC_6H_4NO_2$ (**5**)	361 (2.5)	304		6.0			11
Ru((*E*)-4,4′-C≡CC_6H_4CH═$CHC_6H_4NO_2$)$(PPh_3)_2(\eta$-$C_5H_5)$ (**11a**)	476 (3.0)	356	6.6	15.5	1455 (1464)	232 (234)	45
Ru((*E*)-4,4′-C≡CC_6H_4N═$CHC_6H_4NO_2$)$(PPh_3)_2(\eta$-$C_5H_5)$ (**12a**)	496 (1.4)	379	7.6	14.8	840 (760)	86 (78)	55
Ru((*E*)-4,4′-C≡CC_6H_4CH═$NC_6H_4NO_2$)$(PPh_3)_2(\eta$-$C_5H_5)$		360		16.8			52
Ru((*E*)-4,4′-C≡CC_6H_4N═$NC_6H_4NO_2$)$(PPh_3)_2(\eta$-$C_5H_5)$		409		16.2			89
Ru(C≡$CC_6H_4NO_2$-4)$(PPh_3)_2(\eta$-$C_5H_5)$	460 (8.5)	351			468	96	29[e]
Ru(C≡$CC_6H_4NO_2$-4)$(PMe_3)_2(\eta$-$C_5H_5)$	477 (4.0)	372			248	39	31[e]

[a] Solutions in THF. [b] HRS(EFISH) at 1.06 μm; HRS values ±10%, EFISH values ±15%. [c] HRS(EFISH) experimental data corrected for absorption at 532 nm using the two-level model, with $\beta_0 = \beta[1 - (2\lambda_{max}/1064)^2][1 - (\lambda_{max}/1064)^2]$; damping factors not included. [d] At 1.9 μm. [e] Reference 1.

be considered as β_{vec} ($\beta_{EFISH} = \beta_{HRS} = \beta_{vec} = \beta_{zzz}$). HRS-derived β_{vec} values for **11a**, **12a**, and related acetylide complexes are listed in Table 3. Not surprisingly, chain lengthening as one goes from Ru(C≡$CC_6H_4NO_2$-4)-$(PPh_3)_2(\eta$-$C_5H_5)$ to Ru((*E*)-4,4′-C≡CC_6H_4X═CHC_6H_4-$NO_2)(PPh_3)_2(\eta$-$C_5H_5)$ (X = CH, N) leads to an increased nonlinearity. Phosphine replacement (as one goes from Ru(C≡$CC_6H_4NO_2$-4)$(PMe_3)_2(\eta$-$C_5H_5)$ to Ru(C≡CC_6H_4-NO_2-4)$(PPh_3)_2(\eta$-$C_5H_5)$) leads to a increase in corrected quadratic nonlinearity, but further data are needed to corroborate this result. Although one might expect that the more strongly electron-donating PMe_3 ligand should give rise to increased nonlinearity (our earlier ZINDO-derived nonlinearities showed a small, but not significant, increase in nonlinearity on replacement of PPh_3 by PMe_3),[1] Mulliken analyses of charge density suggest that the ruthenium in the PPh_3 complex is more electron rich than in the PMe_3 complex (+1.40 and +1.47, respectively);[1] this, coupled with a higher extinction coefficient for the MLCT band in the PPh_3 complex (not factored into the two-level correction employed), may be responsible for its higher-than-expected nonlinearity. Both HRS and EFISH suggest a substantial increase in the two-level-corrected β_{vec} value on atom replacement of N by CH in the bridging group; there is a 3-fold increase in quadratic optical nonlinearity at 1.06 μm in proceeding from **12a** to **11a**. The significant difference between **11a** and **12a** is the strength of the MLCT optical transition; the ene-linked acetylide complex has an oscillator strength for this transition more that twice that of the imine-linked analogue. The two-level-corrected β_{vec} value is dependent on the difference in dipole moments between ground and excited states and on extinction coefficients of the relevant transition. Assuming that the excited-state dipoles for **11a** and **12a** are similar, dipole moment differences for **11a** and **12a** will be small, and the 3-fold enhancement in β_0 as one goes from **12a** to **11a** would arise largely from differences in oscillator strength for the dominant transition.

Kanis *et al.* have established the validity of ZINDO-derived second-order optical nonlinearities as an excellent indication of experimentally determined nonlinear optical merit in both organic[20] and organometallic[21] systems. We have previously utilized crystallographically derived atomic coordinates of Ru(C≡CC_6H_4R-4)-$(PR'_3)_2(\eta$-$C_5H_5)$ (R = H, NO_2; R′ = Me, Ph) to obtain β_{vec} and evaluate the significance of phosphine replacement, nitro substituent, and M−C(acetylide) distance on this parameter.[1] We have now extended these studies to embrace the "extended" arylacetylides, which (i) pro-

(20) Kanis, D. R.; Marks, T. J.; Ratner, M. A. *Int. J. Quantum Chem.* **1992**, *43*, 61.
(21) Kanis, D. R.; Ratner, M. A.; Marks, T. J. *J. Am. Chem. Soc.* **1992**, *114*, 10338.

vides a check on the accuracy of ZINDO for complexes which are experimentally accessible and (ii) provides confidence that ZINDO-derived results for "artificial" complexes are meaningful (Table 3). Optical nonlinearities for **5** and **11a** were calculated by utilizing the crystallographically derived coordinates; those of the other "extended" arylacetylides were determined by atom substitution using the geometry of **11a**.

Clearly, the calculated optical nonlinearity of **11a** (45×10^{-30} cm^5 esu^{-1}) is far greater than the sum of those of its precursors $RuCl(PPh_3)_2(\eta\text{-}C_5H_5)$ (1×10^{-30} cm^5 esu^{-1}) and (*E*)-4,4′-$HC{\equiv}CC_6H_4CH{=}CHC_6H_4NO_2$ **(5)** (11×10^{-30} cm^5 esu^{-1}) (although the dihedral angle for the phenyl rings in **5** is 47.5°, a coplanar arrangement results in a calculated β_{vec} of 13×10^{-30} cm^5 esu^{-1}; the computed nonlinearity seems relatively insensitive to this parameter). More importantly, it is about 50% larger than for $Ru(C{\equiv}CC_6H_4NO_2\text{-}4)(PPh_3)_2(\eta\text{-}C_5H_5)$; as with organic molecules, chain lengthening leads to an increase in calculated nonlinear response. Tsunekawa and Yamaguchi[22] have probed the effect of atom variation in the bridging groups of stilbenes and their imine- and azo-linked analogues; decrease in nonlinearity was observed on replacing CH by N, and compounds with nitrogen atoms at the "even-numbered" positions (counted from the electron-accepting nitro group) have larger β values than those compounds with nitrogen at the "odd-numbered" position. For the organometallic system under consideration here, a small *increase* is observed in calculated response on replacing the ene linkage with an imino group. The computed response of the imino complex (**12a**) is slightly larger than that of $Ru(4,4'\text{-}C{\equiv}CC_6H_4CH{=}NC_6H_4NO_2)(PPh_3)_2(\eta\text{-}C_5H_5)$, the same trend that was observed in the purely organic system above. Despite the small increase on replacement of one CH by N, there is a dramatic increase on the second substitution, with the computed response for the azo-linked complex almost double that of **11a**. In contrast, ene-linkage replacement by an azo linkage in the organic system leads to a dramatic *decrease* in molecular first hyperpolarizability.[22] To check the validity of direct atom substitution without other structural manipulation, we extracted representative examples of organic molecules bearing the arylene−X=X−arylene (X = CH, N) structural type from the Cambridge Crystallographic Database and repeated the above calculations using averaged bridging unit bond distances; all calculated responses were within 4×10^{-30} cm^5 esu^{-1} of the tabulated values, the relative ordering was maintained, and the dramatic increase on replacement of an ene with an azo linkage was confirmed. Comparison of the ZINDO-derived β_{vec} value with the two-level-corrected β_{vec} reveals that the former underestimates the experimental nonlinearities; this underestimation would probably be exacerbated if damping were factored into the experimental results. It would be expected, though, that the computationally determined values which approximate gas-phase nonlinearities would be smaller than solution-phase measurements, as dipolar solvents such as $CHCl_3$ will help to stabilize the MLCT excited state for the latter (these complexes undergo positive solvatochromism for the MLCT transition). Recent work examining the solvent effect on second-order nonlinear optical response of π-conjugated organic molecules has shown substantial enhancement of β_{vec} in proceeding from gas phase to polar solvent.[23] Additionally, however, it has not been demonstrated that the two-state model successfully employed to determine static β_0 for simple organic systems has validity for organometallic complexes of the type considered here. Further, the overestimations in ground-state dipole moment and energy of MLCT transition (displacing the latter farther from 532 nm) would both contribute to a decrease in the computed β_{vec} value.

The results described above are consistent with an increase in quadratic optical nonlinearity upon chain lengthening of an organometallic chromophore. More subtle changes (phosphine substitution, bridge variation) require further data to establish their effect upon nonlinearity; studies directed toward these goals are currently underway.

Acknowledgment. We thank the Australian Research Council and Telstra for support of this work and Johnson-Matthey Technology Centre for the generous loan of ruthenium salts. Dr. A. C. Willis is thanked for help with the structure solution and refinement of **11a**. Dr. D. Ollis is thanked for access to an INDY workstation. I.R.W. is the recipient of an Australian Postgraduate Research Award (Industry), and M.G.H. holds an ARC Australian Research Fellowship. S.H. is a Research Assistant of the Belgian National Fund for Scientific Research. Support from the Belgian Government (Grant No. IUAP-16), the Belgian National Science Foundation (Grant No. G.2103.93, 9.0012.92 and 9.0011.92), and the University of Leuven (Grant No. GOA 95/1) is gratefully acknowledged.

Supporting Information Available: Tables giving final values of all refined atomic coordinates, all calculated atomic coordinates, all anisotropic and isotropic thermal parameters, and all bond lengths and angles for **11a**, a plot of ZINDO-derived β_{vec} values as a function of the number of state basis functions, and plots giving comparisons of ZINDO-derived β_{vec} values for structures involving (i) atom replacement in **11a** and (ii) averaged structural data (20 pages). Ordering information is given on any current masthead page.

OM950487Y

(22) Tsunekawa, T.; Yamaguchi, K. *J. Phys. Chem.* **1992**, *96*, 10268.

(23) Dehu, C.; Meyers, F.; Hendrickx, E.; Clays, K.; Persoons, A.; Marder, S. R.; Bredas, J. L. *J. Am. Chem. Soc.* **1995**, *117*, 10127.